LOW FREQUENCY MAGNETIC FIELDS NEAR CHARGING STATIONS FOR ELECTRIC VEHICLES

MILAN ORAVEC[1], PAVOL LIPOVSKY[2]

[1]Faculty of Mechanical Engineering, Technical University of Kosice, Kosice, Slovakia

[2]Faculty of Aeronautics, Technical University of Kosice, Kosice, Slovakia

DOI: 10.17973/MMSJ.2022_10_2022088

e-mail: pavol.lipovsky@tuke.sk

Charging stations (CHS) for electric vehicles (EV) are considered as sources of local magnetic fields (MF). The MF created by the CHS depends mainly on the actual charging power and topology of the electrical components inside the CHS. MF are in technical practice represented by the effective value of the magnetic flux density B_{RMS}. However, the complex view has to consider the resulting MF vector, its components and the corresponding frequency values of the components at the measurement point and also their corresponding time development. The paper presents measurements of MF near the CHS that were performed with the VEMA-04 series magnetometer and 38 kW power drawn from the CHS. The parameters of the magnetic fields were evaluated in both the time and the frequency domains. The aim of this analysis is to point out that evaluating only simple effective value B_{RMS} of MF is not sufficient.

KEYWORDS

low frequency magnetic fields, charging station, electric vehicle, effective value of magnetic flux density, rotating/moving vector of the alternating magnetic field, VEMA-041 magnetometer, DFFT

1 INTRODUCTION

Charging stations (CHS) are creating local magnetic fields (MF) around them. The MF parameters depend on the value of the charging current and on the components/devices topology in the CHS. Effective value of magnetic flux density, B_{RMS} (Root Mean Square) is often used as qualitative description of the MF in technical practice. However, since the MF is a vector field, it is not sufficient to use only effective value for complex description of the MF. Generally, multiple frequency components with different amplitudes can be observed near common technical devices [Ripka 2020] in the measured MF and evaluated with the help of discrete fast Fourier transform (DFFT). The knowledge of vector parameters of the MF allows to create such constructions of CHS that the resulting MF vector is directed away from the area of movement of persons. A lot of the CHS (excluding the high frequency types) are working in the low frequency range of MF during the electric vehicle charging process. This MF is specific from both points of view, the work/occupational hygiene and also the compatibility. The MF is also a source of information about the state of electrical components/devices [Oravec 2019b and 2021], whereas this information is minimally used in the technical diagnostics of the CHS.

The CHS can be legally considered as a stable technological device which has to conform the ICNIRP guidelines and their derivatives in European Union (EU) countries [ICNIRP 1998, ICNIRP 2014]. EU countries, where these normatives/standards are not applied, have valid similar more strict directives for work/occupational hygiene, e.g. SBM 2015 [IBN 2015]. EV in comparison to stable CHS is not considered to be a stable source, even during the charging process it is considered to be a mobile source. However, there are no standards for limit values during the EV charging. For a comparison, the JRC guidelines [Trentadue 2020c] were created for MF in EV, in which measurement places (points) in EV are recommended. The JRC guideline arisen from IEC TS 62764 ed. 1 and is very similar to GB/T 37130-2018. According to these procedures the vehicle should be tested in different operating conditions: stationary, driving, during accelerations and decelerations (±2.5 m/s^2 or more) and during charging, with vehicle electrical systems (lights, wipers, air conditioning, heating, etc.) in their worst-case mode of operation. In these cases, the background MF in the measurement site environment must be less than 10 % of the reference values. Furthermore, both procedures allow measurements on a standard chassis dynamometer without requiring the use of an anechoic chamber. The JRC guidelines serve for relative comparison during selected modes of EV operation on a testing stand. This does not give information about specific states of the CHS in concrete place. This is required by the Directive 2013/35/EU on the Minimum Health and Safety Requirements Regarding the Exposure of Workers to the Risks Arising from Physical Agents (electromagnetic fields) [ECS 2013].

The plurality in opinions on the limit values of CHS MF and neglecting the vector nature of the MF are befitting base to point out the solution of this problem – although the MF is a vector, evaluation takes into account the effective value B_{RMS}, however not the direction and often the phases are in real world neglected. The measurement of the MF is a time-space task, so resolving the MF with its orthogonal components can help to create more interpretable insight.

The measurements of B_{RMS} with the aim on comparison to ICNIRP field values near the CHS were shown in [Trentadue 2020a and 2020b]. During the measurements near the CHS in 0.5 - 1 m heights above the ground [Trentadue 2020b], boundary values of B_{RMS} according to the ICNIRP guidelines were observed to 31 cm distance from the CHS with 132 A current. In works [Novotňák 2021, Oravec 2019a and 2021] was shown the possibility of measurement and evaluation of the MF parameters with consideration of the vector nature of the field. It was presented that more complex view of MF near the CHS is provided by the visualization of the MF vector tip trajectory [Marková 2021], so called rotating/moving vector of the alternating magnetic field (AC MF). From this visualization it is possible to obtain quick insight on scalar parameters and also the vector parameters of the MF.

2 METHODOLOGY AND OBJECTS

2.1 Experimental Method

Local MF near the CHS is created by electric current flowing through components/devices of the CHS and interaction with the construction materials. For this MF it is possible to measure components of magnetic flux density B_x, B_y, B_z, in x, y, z directions of the orthogonal coordinate system. The resulting vector of the MF is given by equation:

$$\vec{B} = \vec{B}_x + \vec{B}_y + \vec{B}_z \quad \text{[T]} \tag{1}$$

This vector changes its magnitude and direction - rotates/moves with its frequency. It can be visualized by the trajectory of the vector tip in the form of line or scatter graph. The magnitude of the resulting vector B_{total} is:

$$B_{total} = \sqrt{B_x^2 + B_y^2 + B_z^2} \quad [\mathrm{T}] \qquad (2)$$

The B_{RMS} value is a scalar quantity computed according to the equation:

$$B_{RMS} = \sqrt{\frac{1}{t_2 - t_1} \int_{t_1}^{t_2} [B(t)]^2 \, dt} \quad [\mathrm{T}] \qquad (3)$$

where t_1 and t_2 are forming the time interval on which the effective value is being evaluated.

The resulting visualization for simple devices, e.g. cable, transformer, in stationary modes of operation, takes the form of the closed patterns [Oravec 2020] with the characteristic carrying frequency. Figure 1(a) shows such example of the visualization of the MF vector tip trajectory identified near a charger during the charging process of 12 V accumulator through the full bridge rectifier. The color scale is blue-red corresponding to minimum and maximum values. The right side of the Figure 1(b) shows the time development and frequency spectrum of one channel in the QtVema software as it was measured by the VEMA-04 series fluxgate magnetometer in the example case.

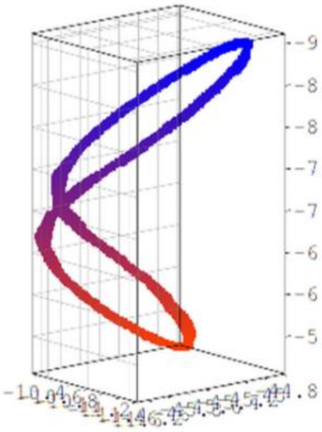

a)

b)

Figure 1. Visualization of magnetic field parameters from VEMA-04 magnetometer in QtVema software

2.2 Measurement Device

The VEMA-041 magnetometer (Figure 2) is a relax-type fluxgate magnetometer operating with conversion of magnetic field measurement into time intervals difference measurement. The device allows to measure 4 vector components of magnetic field simultaneously – there is no multiplexing among the channels, which is necessary for phase analyses. VEMA-04 magnetometers operate with the constant sampling frequency of 1 kHz. Besides the built-in functions of the software that give an insight on the measurements immediately during the measurements (DFFT, autocorrelation, vector tip trajectory), the created files/recordings can be processed also by commercial statistical software or programmed scripts. The sensitivity of the used magnetometer VEMA-04 is approximately 1.7 nT/LSB (Least Significant Bit), the calibration process was realized according to the procedure described in [Kliment 2017]. Full-scale non-linearity is below 0.5 % in the measurement range of ±60 µT. The noise of the magnetometer channel is within ±5 nT in the DC – 250 Hz frequency range according to the experimental method presented in [Praslicka 2017]. The vector sensors are placed in the non-magnetic measurement fixture to create an orthogonal sensing topology – A,B,C channels corresponding to the B_x, B_y, B_z values. The sensors are freely movable and different arrangements can be created, but often the fourth channel is used to monitor the changes in the background field in the chosen direction.

Figure 2. VEMA-04 series magnetometer

2.3 Charging Stations in Experiment

MF near CHS for EV is dependent on the current charging mode/state of the CHS. Several different types of CHS were analyzed during the charging process. Figure 3(a) shows one of the oldest type of CHS.

The charging of EV can be performed by direct current (DC) or alternating current (AC). In case that AC is used, the EV has a built-in AC/DC converter. The most often used CHS with the fast-charging feature, Figure 3(b) and Figure 3(c), allows to charge with the power up to 45 kW for a common EV. During all experiments, the same EV – second generation Nissan Leaf was used, since it is a very common EV.

a) b) c)

Figure 3. Charging stations

3 MAGNETIC FIELD NEAR CHARGING STATION

3.1 *Electric Power Distribution and Transformation*

Processes related to the energy transfer are realized by distribution networks and transformation to required parameters. The transformation is realized in transformers and converters. Typical values of magnetic flux densities for over ground and underground conductors are shown in Table 1.

Group	Voltage [kV]	BRMS [μT]	Frequency [Hz]
Over ground	400	200	50
	110	200	50
	22	4	50
Underground	400	83	50
	110	0.76	50

Table 1. Over ground and underground conductors low frequency magnetic fields [Oravec 2018]

The over ground 400 kV line MF was at 1.5 m distance from the power line capable to carry 2100 A, the 110 kV line MF was in the same distance from the power line capable to carry 1240 A, the 22 kV line MF was in 15 m distance from the power line axis. The underground lines MF were measured at the surfaces of the cables.

3.2 *Magnetic Field near Charging Station with 38kW Power Drawn by the Electric Vehicle*

The measurements of MF near CHS in [Trentadue 2020a, Trentadue 2020b] confirmed reaching of the ICNIRP limit values for stable sources in distance of 31 cm from the CHS during the speed-charging of EV. The charging was performed by AC with 127 A and 132 A with the frequency of 50 Hz.

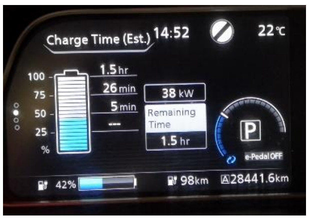

a)

b)

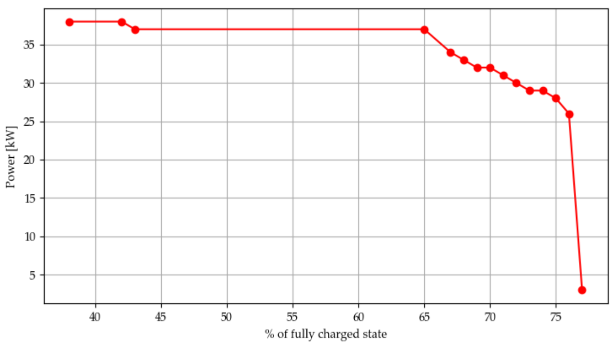

Figure 4. EV charging management (second generation Nissan Leaf)

The peak values of MF depended on the placement of the electronics in the CHS. Our measurements were performed on different CHS, (Figure 3(a-c)), whereas the CHS in Figure 3(c) is the most frequented in Kosice city in Slovakia. Since the results were similar, the analyses results for CHS in Figure 3(c) are presented. An example from the charging process of the second-generation Nissan Leaf EV is shown in Figure 4. Maximum charging power drawn by the vehicle was 38 kW. The magnetic field was measured at 20 cm distance from the face of the CHS housing in heights of 0 cm, 50 cm and 100 cm and on the top of the housing. The x-axis was oriented towards the CHS, y-axis was in the horizontal plane and z-axis was vertically oriented, so the right-hand orthogonal system was created at the measurement point.

The EV charging management is characteristic with two phases. In the first phase, approximately up to the 75-76 % of fully charged state the charging power is set to its maximum and very slowly decreases (Figure 4(a)). After the 75-76 % point the charging power is decreased to 3 kW (Figure 4(b)) and slowly decreases as the accumulator is being fully charged (Figure 4(c)). In this way the accumulator lifetime is preserved as much as possible.

Most of the electronics and power components of the CHS is placed in 50 cm – 100 cm height. Using DFFT on the magnetic field recordings the frequency spectrums were plotted – Figure 5 and Figure 6. The figures show the frequency spectrums in two measurement points at 38 kW charging power – in 50 cm height and 20 cm front distance and on the top of the CHS housing.

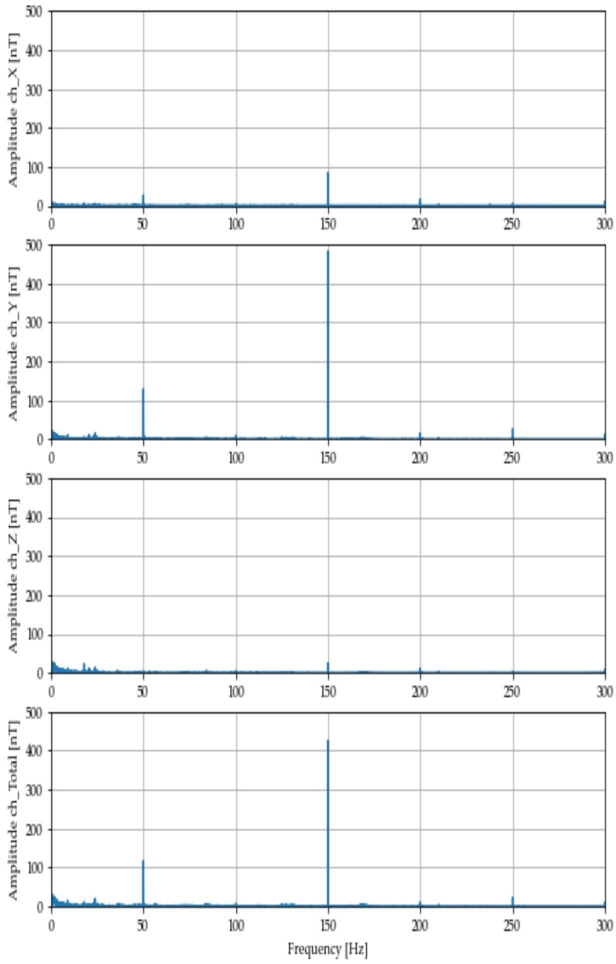

Figure 5. Amplitude frequency spectrums in front of the charging station

From the amplitude frequency spectrums it can be seen that the resulting MF in the measurement point is created by superposition of different electronic components and contains several higher harmonics. The phase differences of MFs created by multiple sources and nonlinearities in components´ characteristics cause formation of not only odd harmonics, but also even harmonics of the 50 Hz base frequency.

The second fact is that B_y was the strongest component and this was confirmed also during charging with reduced power. The position and orientation of the electronic components is the main factor influencing the resulting vector of the MF. Figure 7 and Figure 8 show the MF vector tip trajectory visualization.

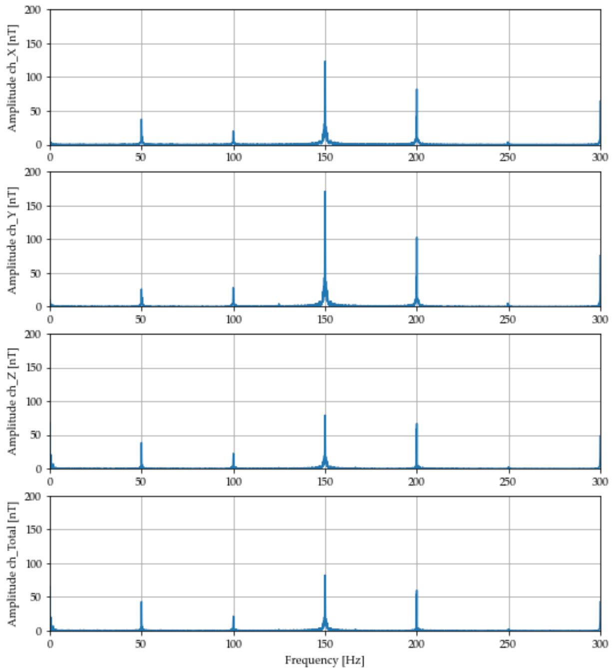

Figure 6. Amplitude frequency spectrums on top of the charging station

The AC components of the MF are within ±800 nT in the Y-axis and below ±400 nT in the X-axis and Z-axis directions in the measurement point in front of the CHS. This is in the agreement with the values shown in Figure 5. The created pattern is considered to be closed and periodic – this is also in agreement with the nature of the charging – it is a cyclic process. As it is shown in Figure 5, the 150 Hz component is relatively high compared to the base industrial frequency of 50 Hz.

The measured values are comparable to the values reached inside an EV according to the researches presented in [Fakhfakh 2016] and [Yang 2019]. Inside an EV are also transposed natural and artificial fields from the urbanized environment, however, the lasting of high currents magnetic fields is not as long as near the CHS. Compared to the research presented in [Gryz 2022] the measured values are lower; however the lower charging current has to be taken into account. Considering the construction of both the CHS and the EV, also material and geometrical properties have to be taken into consideration regarding the shielding effects with respect to the direction and strength of the magnetic field environment, since some of the incidence directions can be considered as easily magnetized.

The graphic patterns can be created with the selected number of samples in the evaluated segment, as it was in our case with a simple script written in the Python programming language. In this way the measurements can be compared and coprocessed with other information provided with e.g. a video recording.

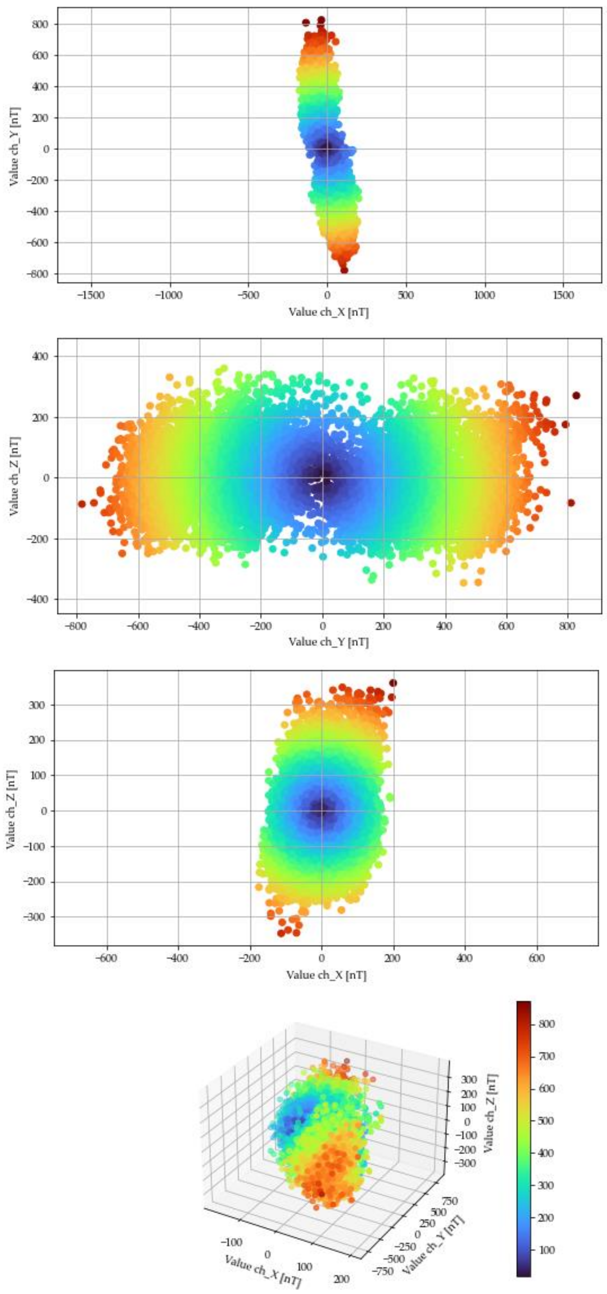

Figure 7. Magnetic field vector visualization in planes and 3D, 10 seconds recording in front of the charging station during charging

A practical example of a bad solution is the placement of the power transformer near the CHS, e.g. in wall behind it. The ICNIRP limits discuss also the d*B*/d*t*, the time change of the MF, which is often neglected when evaluating the CHS. For example, in the industrial workplaces with high MF such as electrolysis workplace, it is necessary to consider the movement of the personnel and the induced fields. Also, the persons with cardio stimulator with operating frequencies in the range from 0.9 Hz to 1.1 Hz should be taken into consideration in the normatives.

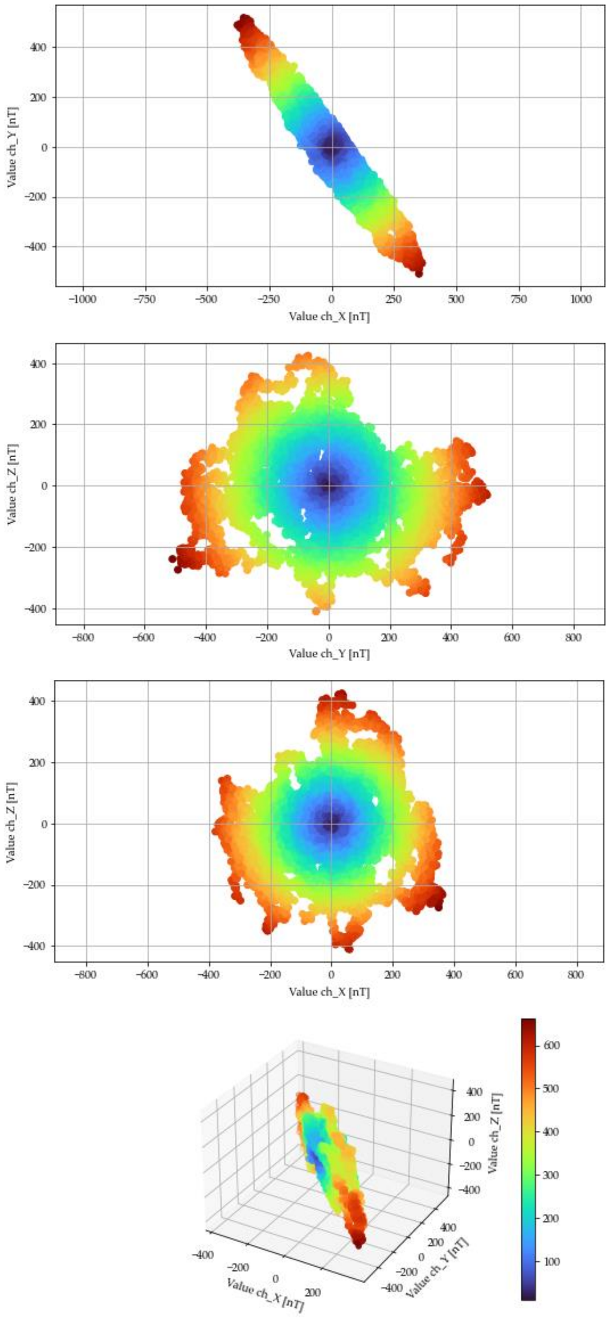

Figure 8. Magnetic field vector visualization in planes and 3D, 10 seconds recording on top of the charging station during charging

4 DISCUSSION

From the results of the realized measurements some conclusions for theoretical and practical knowledge can be drawn.

4.1 Measurement and Evaluation of Magnetic Field near Charging Station

With respect to the vector nature of the magnetic field, the measurements should be performed with vector magnetometers, ideally with simultaneous sampling of the orthogonal magnetic field components, since scalar magnetometers can provide misleading information. A typical example is in Figure 9, where for simplicity 2D case is shown when the total magnetic field stays constant, however, there are two AC components B_x and B_y that have a phase difference of 90°.

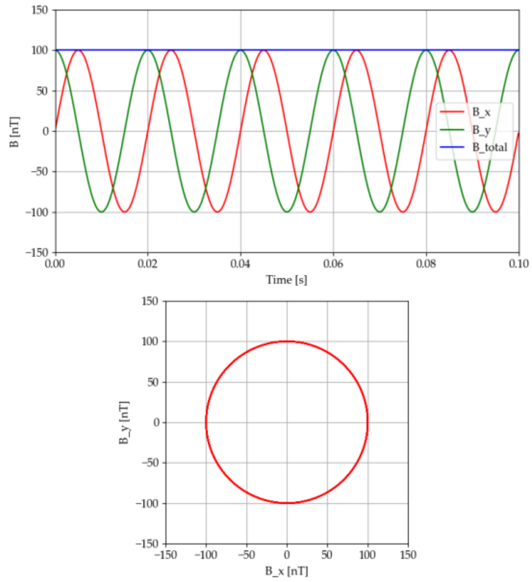

Figure 9. Example of resulting total from two signals with the same amplitude and phase difference of 90°

4.2 Selection of Magnetic Field Parameters of near Charging Station for the Purpose of Dynamic Changes Evaluation

From the Figure 5 and Figure 6 and visualizations in Figure 7 and Figure 8 it is clear, where the main electronics part is placed within the CHS. This fact should be taken into account and the measurements should be performed in 0 cm – 50 cm heights above the ground. The resulting effective value of MF, B_{RMS}, can be computed according to the equation (3). However, considering the character of this value there is missing information about the direction and changes in the MF near the CHS. This value is suitable only for comparison with limit values from ICNIRP guidelines and their national derivatives. The SBM 2015 standard [IBN 2015] created in Germany for the occupational/work hygiene has significantly more strict limit values of MF for administrative and residential buildings. This standard is also recommended by the Austrian Medical Chamber. This kind of standard does not exist in Slovakia and Czech Republic and also in other countries [STAM 2018].

Even if the EV stands still and is charging it is not legally considered to be a stable source. The JRC guidelines [Trentadue 2020c] were created in 2019 for comparison of MFs in EVs. Based on the experiments a standard was specified that indicates places and processes for MF in EV comparison. Such normative for CHSs does not exist in this time.

The obligation to evaluate MFs is given by EU directive 2013/35/EU [ECS 2013] and the MF created by the CHS should be evaluated not only after the manufacturing but also after the placement of the CHS in its specific place. However, this fact is not respected. Vague recommendations in manuals for CHSs are an example. The MF is a vector field and therefore it should be evaluated in such way. Based on the vector measurements it is possible to create standards for CHSs that should be respected before the expedition of the CHS and also after its placement. These measurements can give answers to questions related to:

- identification of the resulting MF vector and its AC components,
- identification of directions in which the MF is minimal and maximal,
- computation of B_{RMS} limit value,
- take a stance to different limit values, since in different countries are adopted different evaluation methods and

limits – this information is important for CHS manufacturers,

- take a stance to electromagnetic compatibility of CHS and possible future devices near them, e.g. security systems.

Considering the possibilities of current MEMS (micro electro-mechanical systems) sensors, it can be stated that their integration into the CHS for online monitoring can provide also shareable information not only about the monitored MFs, but also about the state of the CHS. Monitoring of these changes can make the maintenance process more effective.

4.3 Proposal for Charging Station Placement in Occupational and Administrative Buildings

It is necessary to create unified directive/standard in the European Union for the area of building construction hygiene. The base of such directive can be the SBM 2015 standard created in Germany. This type of normative should have defined the boundary conditions for testing and also for operating of CHS. In the directive [ECS 2013] the requirement for MF measurement of stable (stationary) devices (valid also for CHS) is mentioned – measurements in place of the operation. However, even these days such measurements are very difficult to find if they exist. The knowledge of the MF parameters will allow to take actions for a specific place.

The MF near the CHS is considered even nowadays to be of less importance from the construction point of view. Often it can be sufficient to place the electrical equipment of the CHS in such way that the strong field is directed away from the charging space. The CHS can be optimized by phase-shifting of the fields and geometrical topology of used materials to create minimal MFs, however this requires vector measurements (respecting the vector nature) of MFs.

4.4 Proposal for Standard Measurement of Magnetic Field near Charging Station

The MF near the CHS can be measured already during the manufacturing process and also after the completion in conformity to the Directive 2013/35/EU on the Minimum Health and Safety Requirements Regarding the Exposure of Workers to the Risks Arising from Physical Agents, which also requires knowledge about the MF after the CHS placement in its operational point. The MF measurement can be performed at a circle with 20 cm distance from the CHS (bounded with a described circle) in 8 (16) points in 30 cm intervals from the ground up to the top of the CHS. The measurements should be performed during maximal and reduced charging power with respect to the technical parameters of the CHS. Based on this kind of measurement it is possible to create a map of MF near the CHS for different charging modes.

Intelligent solutions in the form of shared information about the magnitude and direction of MF near the CHS will allow the service personnel to monitor the CHS state in real time and also to get information about the exposition to MF for persons near the CHS based on the chosen standard and limit values.

5 CONCLUSIONS

The vector nature of the magnetic field includes the direction, magnitude and frequency – these components are the minimal parameters that has to be known for concrete design of charging process of an electric vehicle. However, the magnetic field has also other parameters connected to the energy transfer.

The measurement results confirm that the charging stations and electric vehicles are sources of the magnetic fields. The paper presents proposals based on the experimental results on how to solve the measurements for magnetic fields near the charging stations.

Nowadays, the placement of the charging stations is in nature close to the building construction hygiene rather than to the stable/stationary devices with magnetic fields. Current normatives allow to place the charging station on one side of the wall, whereas on the other side of the same wall can be an office, occupied place, a flat and so. For the sources like the transformers and cablings, it is relatively easy to determine most of the magnetic field properties, since they operate with the industrial 50 Hz frequency (and its harmonics). More difficult is the situation when the AC/DC converters are used.

The magnetic field is a unique source of information about changes in states of objects and also about the environment where personnel can move. Current tools used to describe this state are insufficiently used.

In the future, the MEMS (micro electro-mechanic systems) sensors can be built in the CHS and can be used to measure the magnetic fields and share these measurements – thus a new approach not only in technical diagnostics but also in state information of the charging station and its surrounding could be created. In similar way to noise maps and their standards/normatives magnetic field maps for concrete charging modes of an electric vehicle can be created.

The knowledge about the charging station magnetic field properties gives new tools for human protection and prevention into the hands of designers already in the construction design phase of the electric vehicle.

ACKNOWLEDGMENTS

This work was supported by Slovak grant agencies with funding the KEGA 013TUKE4/2020 and APVV-17-0184 projects.

REFERENCES

[ECS 2013] European Committee for Standardization. Directive 2013/35/EU on the Minimum Health and Safety Requirements Regarding the Exposure of Workers to the Risks Arising from Physical Agents (Electromagnetic Fields) [15/3/2022]. European Committee for Standardization: Brussels, Belgium, 2013. Available from: https://eur-lex.europa.eu/legal-content/EN/TXT/PDF/?uri=CELEX:32013L0035&rid=2.

[Fakhfakh 2016] Fakhfakh, M.A. (ed.). Modeling and Simulation for Electric Vehicle Applications. Croatia: InTech, 2016. ISBN 978-953-51-2637-9.

[Gryz 2022] Gryz, K., Karpowicz, J. and Zradziński, P. Complex Electromagnetic Issues Associated with the Use of Electric Vehicles in Urban Transportation. Sensors, 2022, Vol. 22, No. 5, 1719. DOI: https://doi.org/10.3390/s22051719.

[IBN 2015] Institut für Baubiologie + Nachhaltigkeit IBN. Standard of Building Biology Testing Methods, SBM-2015 [11/3/2022]. Available from: https://buildingbiology.com/site/downloads/standard-2015-englisch.pdf.

[ICNIRP 1998] International Commission on Non-Ionizing Radiation Protection (ICNIRP). Guidelines for Limiting Exposure to Time-Varying Electric, Magnetic, and Electromagnetic Fields (up to 300 GHz). Health Phys., 1998, Vol. 74, No. 4, pp. 494-522.

[ICNIRP 2014] International Commission on Non-Ionizing Radiation Protection (ICNIRP). Guidelines for Limiting Exposure to Electric Fields Induced by Movement of the Human Body in a static magnetic fields and by time-varying magnetic fields below 1 Hz. Health Phys., 2014, Vol. 106, No. 3, pp. 418-425.

[Kliment 2017] Kliment, T., Praslicka, D., Lipovsky, P., Draganova, K. and Zavodsky, O. Calibration of Magnetometerfor Small Satellites Using Neural Network. Acta Phys. Pol. A, 2017, Vol. 131, No. 4, pp. 1129-1131. DOI: https://doi.org/10.12693/APhysPolA.131.1129.

[Markova 2021] Markova, I., Oravec, M., Osvaldova, L.M., Sventekova, E. and Jurc, D. Magnetic Fields of Devices during Electric Vehicle Charging: A Slovak Case Study. Symmetry, 2021, Vol. 13, No. 11, 1979. DOI: https://doi.org/10.3390/sym13111979.

[Novotnak 2021] J. Novotnak, J., Oravec, M., Hijj, J. and Jurc, D. Slip Control by Identifying the Magnetic Field of the Elements of an Asynchronous Motor. In: Proc. of the IEEE 19th World Symp. on Applied Machine Intelligence and Informatics (SAMI), Herlany, Slovakia, 21-23 January 2021, IEEE, pp. 0273-0278. DOI: doi.org/10.1109/SAMI50585.2021.9378658.

[Oravec 2018] Oravec, M., Lipovsky, P. and Smelko, M. Low Frequency Magnetic Fields in Work Environment (in Slovak). Ostrava: SPBI, 2018.

[Oravec 2019a] Oravec, M., Pacaiova, H., Izarikovs, G. and Hovanec, M. Magnetic Field Image—Source of Information for Action Causality Description. In: Proc. of the 2019 IEEE 17th World Symposium on Applied Machine Intelligence and Informatics (SAMI), Herlany, Slovakia, 24–26 January 2019, IEEE, pp. 0101-0105, ISBN 978-1-7281-0250-4. DOI: https://doi.org/10.1109/SAMI.2019.8782747.

[Oravec 2019b] Oravec, M., Draganova, K., Lipovsky, P., Smelko, M. and Bugar, T. UV 8860. Device for Slip Control by Identifying the Magnetic Field of Elements of an Asynchronous Motor with a Frequency Converter. Utility Model 8860 [3rd January 2022]. Available online: http://wbr.indprop.gov.sk/WebRegistre/UzitkovyVzor/Detail/50040-2019.

[Oravec 2020] Oravec, M., Draganova, K., Lipovsky, P., Witos, M. and Smelko M. Low Frequency Magnetic Field – Instruments, Measurements, New Technologies (in Slovak). Ostrava: SPBI, 2020.

[Oravec 2021] Oravec, M., Lipovsky, P., Smelko, M., Adamcik, P., Witos, M. and Kwasniewski, J. Low-Frequency Magnetic Fields in Diagnostics of Low-Speed Electrical and Mechanical Systems. Sustainability, 2021, Vol. 13, No. 16, 9197. DOI: https://doi.org/10.3390/su13169197.

[Praslicka 2017] Praslicka, D., Lipovsky, P., Hudak, J. and Smelko, M. Estimation of multichannel magnetometer noise floor in ordinary laboratory conditions. Acta Phys. Pol. A, 2017, Vol. 131, No. 4, pp. 1123-1125. DOI: https://doi.org/10.12693/APhysPolA.131.1123.

[Ripka 2020] Ripka, P., Blažek, J., Mirzaei, M., Lipovsky, P., Smelko, M. and Draganová, K. Inductive Position and Speed Sensors. Sensors, 2020, Vol. 20, No. 1, 65. DOI: https://doi.org/10.3390/s20010065.

[Stam 2018] Stam, R. Comparison of international policies on electromagnetic fields (power frequency and radiofrequency fields) [1st May 2022]. Bilthoven: National Institute for Public Health and the Environment, RIVM, Netherlands, 2018. Available from: https://www.jrseco.com/wp-content/uploads/Comparison-of-international-policies-on-electromagnetic-fields-2018.pdf.

[Trentadue 2020a] Trentadue, G., Pinto, R., Salvetti, M., Zanni, M., Pliakostathis, K., Scholz, H. and Martini, G. Assessment of Low-Frequency Magnetic Fields Emitted by DC Fast Charging Columns. Bioelectromagnetics, 2020, Vol. 41, No. 4, pp. 308-317. DOI: https://doi.org/10.1002/bem.22254.

[Trentadue 2020b] Trentadue, G., Pinto, R., Zanni, M., Scholz, H., Pliakostathis, K. and Martini, G. Low Frequency Magnetic Fields Emitted by High-Power Charging Systems. Energies, 2020, Vol. 13, No. 7, 1594. DOI: https://doi.org/10.3390/en13071594.

[Trentadue 2020c] Trentadue, G., Zanni, M. and Martini, G. Assessment of low frequency magnetic fields in electrified vehicles. JRC120312. Luxembourg: Publications Office of the European Union, 2020. DOI: https://doi.org/10.2760/056116.

[Yang 2019] Yang, L., Lu, M., Lin, J., Li, C, Zhang, Ch., Lai, Z. and Wu, T. Long-Term Monitoring of Extremely Low Frequency Magnetic Fields in Electric Vehicles. International Journal of Environmental Research and Public Health, 2019, Vol. 16, No. 19, 3765. DOI: https://doi.org/10.3390/en13071594.

CONTACTS:

Prof. Ing. Milan Oravec, PhD.
Technical University of Kosice, Faculty of Mechanical Engineering,
Department of Safety and Quality
Letna 9, 042 00 Kosice, Slovak Republic
milan.oravec@tuke.sk

Assoc. Prof. Ing. Pavol Lipovsky, PhD.
Technical University of Kosice, Faculty of Aeronautics,
Department of Aviation Technical Studies,
Rampova 7, 040 01 Kosice, Slovak Republic
pavol.lipovsky@tuke.sk